ChemComm

Accepted Manuscript

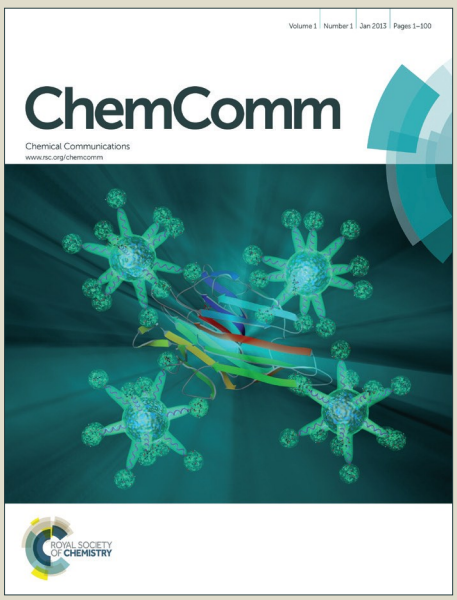

ROYAL SOCIETY OF CHEMISTRY

www.rsc.org/chemcomm

Journal Name

COMMUNICATION

Enhancing the Plasmonic Circular Dichroism by Entrapping Chiral Molecules at the Core-Shell Interface of Rod-Shaped Au@Ag Nanocrystals†

Received 00th January 20xx,
Accepted 00th January 20xx

DOI: 10.1039/x0xx00000x

www.rsc.org/

Shuai Hou,[a,b] Jiao Yan,[a,b] Zhijian Hu[a] and Xiaochun Wu*[a]

We report the enhancement of plasmonic circular dichroism (PCD) in cysteine-modified Au nanorods via Ag coating. The entrapment of cysteine at the Au-Ag interface effectively amplifies the local electromagnetic field and leads to a strong enhancement of the PCD response. Ag coating on sphereical nanoparticles modified with cysteine does not generate obvious PCD signals.

Metallic nanostructures support localized surface plasmons, which are the collective oscillation of the conduction electrons coupled to the electromagnetic field. The localized plasmons can interact strongly with molecules,[1] enabling various applications, such as the surface-enhanced Raman spectroscopy, metal-enhanced fluorescence, and localized surface plasmon resonance (LSPR) sensing.[2] Most recently, the study of plasmon–molecule interaction begins to cover chiral molecules.[3] Chiral molecules show circular dichroism (CD), that is, different absorption of left- and right-circularly polarized light, in their absorption bands. According to theoretical predictions,[4] metal nanoparticles coupled to chiral molecules exhibit new CD bands at the LSPR wavelength, even when the chiral molecule and the metal nanostructure are far off resonance. This plasmonic CD (PCD) is due to the Coulomb interaction between the chiral molecules and the nanoparticles.[4] This prediction has been confirmed in several experiments.[5–7] Different kinds of chiral molecules such as peptides[6] and DNA[7] were adsorbed on the surface of metal nanoparticles, leading to weak but definite CD bands around the LSPR wavelength. Further theoretical calculations[8] and experiments[9–13] revealed that the PCD signals can be enhanced by placing the chiral molecules in an electromagnetic hot spot. However, nanoparticle aggregates or assemblies, which support such hot spots, often adopt a chiral configuration under the influence of chiral molecules.[14–16] This will produce PCD effect due to plasmon–plasmon coupling, which is distinct from the Coulomb interaction between plasmon and chiral molecules.[17,18] In fact, there is a debate on the origin of PCD effect supported by the side-by-side assemblies of Au nanorods.[14,16,19] Therefore, it is desirable to achieve large PCD response using discrete nanoparticles, which makes it easier to identify the real origin of the PCD signals, thus providing a better platform for the study of plasmon–chiral molecule interactions.

Herein, we propose a method for the enhancement of PCD in discrete nanoparticle systems, where chiral molecules are embedded inside metal nanocrystals (NCs). Enhanced PCD signals were observed when the chiral cysteine (Cys) molecules were embedded at the core-shell interface of Au@Ag NCs. Several control experiments proved the entrapment of the chiral molecules. Finally, spherical nanoparticles were used to replace the nanorods, but no obvious PCD signals were obseved, highlighting the importance of shape anisotropy in the induction of large PCD signals.

It was reported that some small molecules can be embedded in core-shell metal nanoparticles.[20] These molecules have a mercapto group binding to the core, and an additional group (COOH or NH_2) interacting with the shell. We used a similar method for the entrapment of Cys at the interface of Au nanorods and Ag shells. As shown in Figure 1a, Au nanorods ([Au^0] = 0.1 mM) dispersed in 10 mM CTAB solution were first modified with 20 μM L- or D-Cys through the Au-S bonds, and then a calculated amount of $AgNO_3$ solution (with Ag/Au ratios ranging from 0.5 to 2.0) was added and was reduced by ascorbic acid (AA) under 70°C to form the core-shell Au@Ag NCs (Figure 1a). The existence of Cys obviously accelerated the Ag deposition on the Au nanorods, and the Ag overgrowth completed within 30 min (Figure S1, ESI†). The resulted NCs are rice-like (Figures 1b and S2, ESI†), different from the cuboid shape if no Cys molecules were added.[21] High-resolution TEM images show that these NCs are single crystalline (Figure S3, ESI†). No obvious cavities at the Au-Ag interface was directly observed in the TEM images, but we will prove the entrapment of chiral molecules as will be shown afterwards. With the increasing amount of Ag, the

[a] CAS Key Laboratory of Standardization and Measurement for Nanotechnology, National Center for Nanoscience and Technology, Beijing 100190, China.
[b] University of the Chinese Academy of Sciences, Beijing 100049, China.

† Electronic Supplementary Information (ESI) available: Detailed experimental methods and numerical calculations. See DOI: 10.1039/x0xx00000x

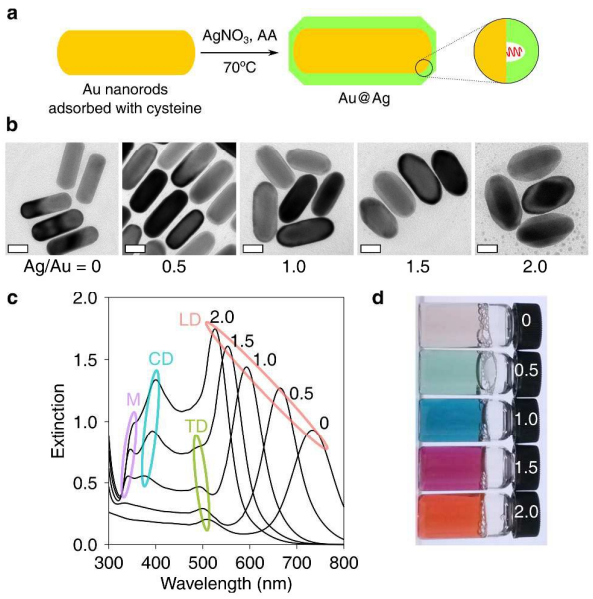

Figure 1. Synthesis and characterization of the Au@Ag nanocrystals (NCs) grown from the cysteine-modified Au nanorods. (a) Schematic of the preparation method. (b) TEM images of the NCs with different Ag/Au ratios ranging from 0 (pure Au nanorods) to 2.0 (scale bar = 20 nm). (c) Extinction spectra. The ellipses denote the four LSPR modes: longitudinal dipole (LD) mode, transverse dipole (TD) mode, corner dipole (CD) mode, and multipole (M) mode. (d) Digital picture of the NC solutions.

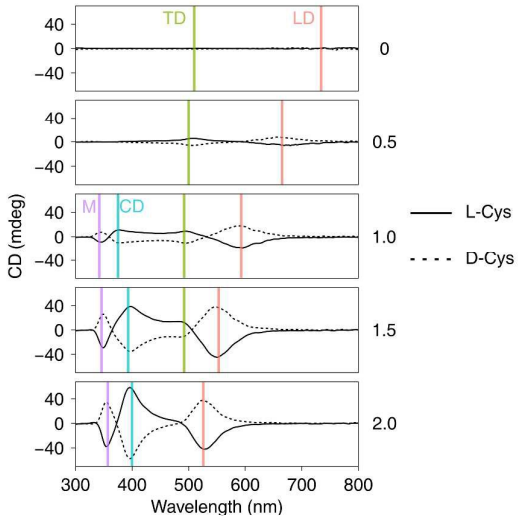

Figure 2. CD spectra of the Au@Ag NCs grown from the cysteine-modified Au nanorods. The vertical lines indicate the LSPR wavelengths, which are directly read from the extinction spectra shown in Figure 1c.

width of the nanorods grew much faster than the length. According to the TEM measurements (Table S1, ESI†), when the Ag/Au ratio is 2.0, the width of the rods increased by 17.5 nm, whereas the length increased by only 3.2 nm. Similar growth behavior was previously reported for the Au overgrowth on Cys-modified Au nanorods.[22] It has been shown that Cys molecules are mainly concentrated on the ends of the Au nanorods, which makes the shell growth on the two ends much slower than the growth on the side.[22]

The coating of Ag greatly modified the spectral features of the Au nanorods (Figure 1c), leading to a dramatic color change of the nanocrystal solutions (Figure 1d). The original Au nanorods exhibited a longitudinal dipole mode at 735 nm and a transverse dipole mode at 510 nm. After the Ag overgrowth, both the longitudinal and the transverse dipole modes were blue-shifted. Two new peaks emerged in the shorter wavelength region as the Ag/Au ratio exceeds 1.0. Numerical calculations (Figure S4, ESI†) revealed that the peak around 340 nm corresponds to a multipole mode, and the peak around 400 nm is a corner dipole mode. Both modes increase in intensity and experience minor red-shift as the Ag shell grows thicker.

The original Au nanorods modified with L- or D-Cys do not exhibit obvious CD signals; however, well-defined CD bands emerged beyond the UV region after coating Ag (Figure 2). There is a one-to-one correspondence between the CD bands and the extinction bands. With the increase of Ag thickness, CD bands corresponding to the longitudinal and transverse dipole modes are blue-shifted and become more intense, and those corresponding to the corner dipole and multipole modes emerge when the Ag/Au ratio reaches 1.0 and continues growing with a thicker shell of Ag. These changes in the CD bands are consistent with the changes in extinction spectra. CD bands of different LSPR modes show different signs. Specifically for the L-Cys case, the longitudinal dipole and the multipole modes exhibit a negative Cotton effect, while the transverse dipole and the corner dipole modes exhibit a positive Cotton effect. The different signs reflect different interfering patterns of electromagnetic fields inside the NCs.[4] In addition, the CD spectrum below 300 nm also experienced an enhancement after coating Ag (Figure S5, ESI†).

The PCD intensity is dependent on the concentrations of the chiral molecules. L-Cys with a concentration of 5 μM induced a PCD signal around 5 mdeg, while L-Cys with concentrations from 10 μM to 40 μM led to PCD signals around 40 mdeg (Figure S6, ESI†). The maximum anisotropic factor in this study is 1.3×10^{-3} (Figure S7, ESI†). The PCD signal is also sensitive to the type of the chiral molecules. We tested two L-Cys derivatives, *N*-acetyl-L-cysteine and L-cysteine methyl ester (Figure S8, ESI†). The former induced PCD signals weaker than L-Cys, and the PCD bands had the opposite signs compared with the L-Cys case. The latter did not lead to an obvious CD signal. This distinction is believed to result from different adsorption conformation on the Au nanorod surface.[23]

To prove that the chiral molecules are embedded in the NCs, we first illustrate that it cannot display as large PCD signals as shown in Figure 2 if the Au@Ag NCs are adsorbed with L- or D-Cys on their surface. We synthesized two kinds of Au@Ag NCs with either a cuboid shape or an arrow shape (see ESI† for preparation methods). The Ag/Au ratios were both 1.5. After incubating with 20 μM L-Cys at 70°C for 30 min, we observed only very weak PCD signals (less than 2 mdeg, see Figure 3). Conversely, if Cys was pre-modified on the Au nanorods, growing a Au shell with irregular shapes can also

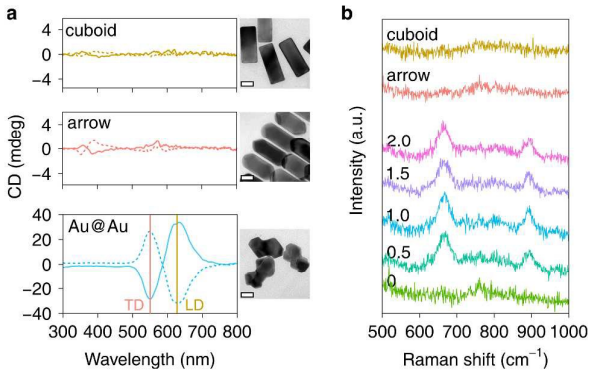

Figure 3. Cys-modification after Ag growth vs. Cys-modification before Ag growth. (a) CD spectra of Au@Ag NCs (cuboids and arrows) with Cys adsorbed on their surfaces and Au@Au NCs grown from Cys-modified Au nanorods. Solid and dotted lines represent L- and D-Cys, respectively. TEM images of the Au@Ag and Au@Au NCs are also shown (scale bar = 20 nm). (b) Raman spectra of L-Cys in Au@Ag NCs (cuboids and arrows) with L-Cys on their surfaces and Au@Ag NCs grown from L-Cys-modified Au nanorods (Ag/Ag ratio ranging from 0 to 2.0).

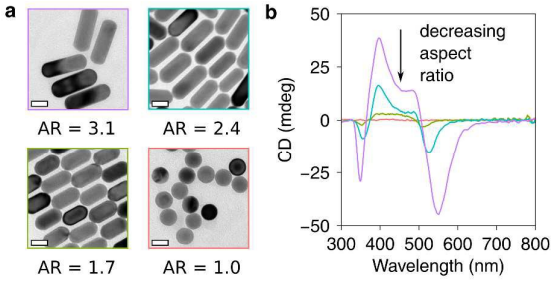

Figure 4. Influence of shape anisotropy on PCD. (a) TEM images of Au nanorods with decreasing aspect ratios (scale bar = 20 nm). (b) CD spectra of the Au@Ag NCs (Ag/Au ratio = 1.5) grown from the Au nanorods shown in (a). The concentration of L-Cys was all 20 μM.

lead to strong PCD signals (Figures 3). Note that the two PCD bands also have a one-to-one correlation with the extinction bands. In the TEM image with a higher amplification, we can observe some discrete cavities inside the Au@Au NCs (Figure S9, ESI†). These results are the first hint that Cys molecules responsible for the PCD signal are not on the surface but embedded inside the NCs.

Next, Raman spectroscopy further suggest that some chiral molecules were entrapped inside the NCs. One of the most notable characteristic of the embedded molecules is their unusually enhanced Raman signal.[20,24,25] We compared the Raman signal of Cys adsorbed on Au@Ag cuboids, Au@Ag arrows, and those grown from Cys-modified Au nanorods. Since the Raman cross section of Cys is very small, we did not observe any characteristic Raman signals in the cuboids and arrows. However, characteristic Raman bands of Cys were observed in NCs grown from L-Cys-modified Au nanorods. The large Raman signal enhancement reflects the intense electromagnetic field around the chiral molecules, which in principle should also play a part in the enhancement of PCD signals.[8]

For another proof of the entrapment of chiral molecules, we used ligand-exchange reaction on the surface of the NCs. Au@Ag NCs exhibiting large PCD signals were first prepared with 20 μM L-Cys. Then the NCs were incubated with 20 μM D-Cys at 70°C for 30 min. No decrease of the PCD signal was observed (Figure S10, ESI†), suggesting that the Cys molecules that induced the PCD signal are not on the surface of the NCs.

For further information of where the chiral molecules are embedded inside the NCs, we adjusted the pH of the Au nanorod solution and found that the nanorods underwent end-to-end assemblies[26] (Figure S11, ESI†). This indicates that the Cys molecules preferentially adsorbed on the two ends of the nanorods, consistent with the previous reports.[22,27,28] Cys can also be specifically modified on the sides of Au nanorods by blocking the two ends with long-chain thiols.[29] However, the PCD signals after Ag coating were much weaker (Figure S12, ESI†), indicating that the PCD signals shown in Figure 2 are mainly from Cys molecules on the ends of the Au nanorods.

Finally, we investigated the influence of anisotropy on the generation of large PCD signals. Anisotropy is an especially important factor in the creation of PCD. For example, theoretical studies has revealed that the PCD signal averages to zero when chiral molecules form a homogeneous shell outside a spherical metal nanoparticle, whereas a nonzero signal is predicted for elongated metal nanoparticles.[30] To obtain nanoparticles with different shape anisotropy, we prepared Au nanorods with decreasing aspect ratios by oxidative etching (Figure 4a).[31] After adding 20 μM L-Cys and coating Ag, the resulted Au@Ag NCs showed reducing PCD signals with decreasing aspect ratio of Au nanorods (Figure 4). In particular, spherical NCs exhibited no obvious PCD signals. Two related reports demonstrated that spherical Au@Ag core-shell nanoparticles can also show quite large PCD signals.[32,33] These nanoparticles have different structures from ours. In the first report, DNA molecules were entrapped at the grain boundaries of the polycrystalline shell.[32] In the second, Cys molecules were in the 0.5 nm gap between the Au core and the Ag shell.[33] It will be interesting to investigate if we can improve the PCD signals in these two systems by using Au nanorods as the core. In addition, we tried coating Ag on Cys-modified Au octahedra with sharp edges and corners. There were clear PCD signals corresponding to the extinction bands (Figure S13†). However, the PCD intensity was much smaller than that in the Au nanorod case, which we believe is due to the weaker geometrical anisotropy of the octahedra.

In conclusion, when Ag is coated on the Cys-modified Au nanorods, some Cys molecules are embedded at the core-shell interface, and the embedded Cys induces strong PCD signals. The strong electric field around Cys, as revealed in the Raman spectra, is believed to be the key factor in PCD enhancement. Meanwhile, no obvious PCD signals were observed in spherical core-shell nanoparticles, highlighting that the anisotropic nanoparticles are better candidates for supporting PCD than their isotropic counterparts. The enhancement of PCD

reported herein, together with the enhancement of Raman scattering reported previously,[20,24,25] establishes that embedding molecules inside metals is an effective method for the enhancement of molecule–plasmon interactions. This method will also benefit the design of PCD-based sensors.

The work was supported by the National Key Basic Research Program of China (2011CB932802) and the National Natural Science Foundation of China (Grant No. 91127013). We also thank Professor Minghua Liu for helpful discussions.

Notes and references

1 H. J. Chen, T. Ming, L. Zhao, F. Wang, L.-D. Sun, J. F. Wang and C.-H.Yan, *Nano Today*, 2010, **5**, 494.
2 M. D. Sonntag, J. M. Klingsporn, A. B. Zrimsek, B. Sharma, L. K. Ruvuna and R. P. Van Duyne, *Chem. Soc. Rev.*, 2014, **43**, 1230.
3 A. Ben-Moshe, B. M. Maoz, A. O. Govorov and G. Markovich, *Chem. Soc. Rev.*, 2013, **42**, 7028.
4 A. O. Govorov, Z. Y. Fan, P. Hernandez, J. M. Slocik and R. R. Naik, *Nano Lett.*, 2010, **10**, 1374.
5 J.-M. Ha, A. Solovyov and A. Katz, *Langmuir*, 2009, **25**, 153.
6 J. M. Slocik, A. O. Govorov and R. R. Naik, *Nano Lett*, 2011, **11**, 701.
7 F. Lu, Y. Tian, M. Z. Liu, D. Su, H. Zhang, A. O. Govorov and O. Gang, *Nano Lett.*, 2013, **13**, 3145.
8 H. Zhang and A. O. Govorov, *Phys. Rev. B*, 2013, **87**, 075410.
9 M. E. Layani, A. Ben Moshe, M. Varenik, O. Regev, H. Zhang, A. O. Govorov and G. Markovich, *J. Phys. Chem. C*, 2013, **117**, 22240.
10 Z. Li, Z. Zhu, W. Liu, Y. Zhou, B. Han, Y. Gao and Z. Tang, *J. Am. Chem. Soc.*, 2012, **134**, 3322.
11 Z. Zhu, W. Liu, Z. Li, B. Han, Y. Zhou, Y. Gao and Z. Tang, *ACS Nano*, 2012, **6**, 2326.
12 R. Y. Wang, P. Wang, Y. Liu, W. Zhao, D. Zhai, X. Hong, Y. Ji, X. Wu, F. Wang, D. Zhang, W. Zhang, R. Liu and X. Zhang, *J. Phys. Chem. C*, 2014, **118**, 9690.
13 V. A. Gerard, Y. K. Gun'ko, E. Defrancq and A. O. Govorov, *Chem. Commun.*, 2011, **47**, 7383.
14 S. Hou, T. Wen, H. Zhang, W. Q. Liu, X. N. Hu, R. Y. Wang, Z. J. Hu and X. C. Wu, *Nano Res.*, 2014, **7**, 1699.
15 X. L. Wu, L. G. Xu, L. Q. Liu, W. Ma, H. H. Yin, H. Kuang, L. B. Wang, C. L. Xu and N. A. Kotov, *J. Am. Chem. Soc.*, 2013, **135**, 18629.
16 W. Ma, H. Kuang, L. B. Wang, L. G. Xu, W.-S. Chang, H. N. Zhang, M. Z. Sun, Y. Y. Zhu, Y. Zhao, L. Q. Liu, C. L. Xu, S. Link and N. A. Kotov, *Sci. Rep.*, 2013, **3**, 1934.
17 B. Auguie, J. Lorenzo Alonso-Gomez, A. Guerrero-Martinez and L. M. Liz-Marzan, *J. Phys. Chem. Lett.*, 2011, **2**, 846.
18 T. Wu, J. Ren, R. Y. Wang and X. D. Zhang, *J. Phys. Chem. C*, 2014, **118**, 20529.
19 B. Han, Z. N. Zhu, Z. T. Li, W. Zhang and Z. Y. Tang, *J. Am. Chem. Soc.*, 2014, **136**, 16104.
20 Y. H. Feng, Y. Wang, H. Wang, T. Chen, Y. Y. Tay, L. Yao, Q. Y. Yan, S. Z. Li and H. Y. Chen, *Small*, 2012, **8**, 246.
21 K. Park, L. F. Drummy and R. A. Vaia, *J. Mater. Chem.*, 2011, **21**, 15608.
22 X. Kou, S. Zhang, Z. Yang, C. K. Tsung, G. D. Stucky, L. Sun, J. Wang and C. Yan, *J. Am. Chem. Soc.*, 2007, **129**, 6402.
23 P. Řezanka, K. Záruba and V. Král, *Colloid. Surface. A*, 2011, **374**, 77.
24 K. D. Beer, W. Tanner and R. L. Garrell, *J. Electroanalytical Chem.*, 1989, **258**, 313.
25 H. Naor and D. Avnir, *J. Mater. Chem. C*, 2014, **2**, 7768.
26 W. H. Ni, R. A. Mosquera, J. Perez-Juste and L. M. Liz-Marzan, *Phys. Chem. Lett.*, 2010, **1**, 1181.
27 K. K. Caswell, J. N. Wilson, U. H. F. Bunz and C. J. Murphy, *J. Am. Chem. Soc.*, 2003, **125**, 13914.
28 H. Nakashima, K. Furukawa, Y. Kashimura and K. Torimitsu, *Chem. Commun.*, 2007, 1080.
29 S. Hou, H. Zhang, J. Yan, Y. Ji, T. Wen, W. Liu, Z. Hu and X. Wu, *Phys. Chem. Chem. Phys.*, 2015, **17**, 8187.
30 A. O. Govorov and Z. Fan, *ChemPhysChem*, 2012, **13**, 2551.
31 C.-K. Tsung, X. S. Kou, Q. H. Shi, J. P. Zhang, M. H. Yeung, J. F. Wang and G. D. Stucky, *J. Am. Chem. Soc.*, 2006, **128**, 5352.
32 X. Wu, L. Xu, W. Ma, L. Liu, H. Kuang, W. Yan, L. Wang and C. Xu, *Adv. Func. Mater.*, 2015, **25**, 850.
33 C. Hao, L. Xu, W. Ma, X. Wu, L. Wang, H. Kuang and C. Xu, *Adv. Func. Mater.*, 2015, **25**, 5816.